Geomorphology 107 (2009) 275–284

Contents lists available at ScienceDirect

Geomorphology

journal homepage: www.elsevier.com/locate/geomorph

Climate change effects on landslides along the southwest coast of British Columbia

Matthias Jakob [a,*], Steven Lambert [b,1]

[a] BGC Engineering Inc., 500-1045 Howe Street, Vancouver, Canada V6Z 2A9
[b] Canadian Centre for Climate Modelling and Analysis, Environment Canada, University of Victoria, P.O. Box 1700, STN CSC, Victoria, B.C., Canada V8W 2Y2

ARTICLE INFO

Article history:
Received 16 May 2008
Received in revised form 19 December 2008
Accepted 22 December 2008
Available online 1 January 2009

Keywords:
Landslides
Debris flows
Climate change
Rainfall intensity
Antecedent rainfall

ABSTRACT

Antecedent rainfall and short-term intense rainfall both contribute to the temporal occurrence of landslides in British Columbia. These two quantities can be extracted from the precipitation regimes simulated by climate models. This makes such models an attractive tool for use in the investigation of the effect of global warming on landslide frequencies.

In order to provide some measure of the reliability of models used to address the landslide question, the present-day simulation of the antecedent precipitation and short-term rainfall using the daily data from the Canadian Centre for Climate Modelling and Analysis model (CGCM) is compared to observations along the south coast of British Columbia. This evaluation showed that the model was reasonably successful in simulating statistics of the antecedent rainfall but was less successful in simulating the short-term rainfall. The monthly mean precipitation data from an ensemble of 19 of the world's global climate models were available to study potential changes in landslide frequencies with global warming. Most of the models were used to produce simulations with three scenarios with different levels of prescribed greenhouse gas concentrations during the twenty-first century. The changes in the antecedent precipitation were computed from the resulting monthly and seasonal means. In order to deal with models' suspected difficulties in simulating the short-term precipitation and lack of daily data, a statistical procedure was used to relate the short-term precipitation to the monthly means.

The qualitative model results agree reasonably well, and when averaged over all models and the three scenarios, the change in the antecedent precipitation is predicted to be about 10% and the change in the short-term precipitation about 6%. Because the antecedent precipitation and the short-term precipitation contribute to the occurrence of landslides, the results of this study support the prediction of increased landslide frequency along the British Columbia south coast during the twenty-first century.

1. Introduction

The scientific consensus that the Earth's surface and oceans are warming at rates unprecedented in the historical record is overwhelming. The latest summary report of the Intergovernmental Panel for Climate Change, (IPCC, 2007) has reasserted and strengthened the observation that the majority of the documented warming in the past century is from anthropogenic greenhouse gas emissions. According to the IPCC, warming will continue even if drastic emission controls are implemented.

A broad consensus also prevails in the scientific community that global warming will have profound effects on the hydrologic cycle (IPCC, 2007). In simple terms, a warming atmosphere and warmer ocean surface temperatures will result in higher rates of evaporation. Higher moisture content in the atmosphere at higher temperatures will result in more energy and more intensive storms over the ocean and coastal areas in the midlatitudes. Inland, the picture becomes more complicated. Precipitation forecasts are fraught with difficulty as precipitation is a second-order effect of global warming and the spatial resolution of global circulation models (GCMs) does not yet account for complex topography, which strongly influences the precipitation regime in south coastal British Columbia.

Although most landslides are triggered by hydroclimatic events, such as prolonged or intensive rain, the following mechanisms are also known to trigger landslides: seismic triggers (particularly for rockfall and rock avalanches); wind (particularly rockfall triggered by root wad leverage); and freeze–thaw cycles (particularly rock fall triggered by the thermal expansion of ice in cracks or the freezing of an exposed face followed by rapid warming creating hydrostatic pressures behind the frozen rock face). Furthermore, landslide frequency can be influenced by anthropogenic activities (such as clearcutting or replanting of trees, forest road construction, or deactivation), as well as by natural factors (such as wind throw, beetle infestations, and forest fires). In the study area (Fig. 1), only the forest activities are relevant. Wind throw, beetle infestations, and

* Corresponding author. Tel.: +1 604 629 3842; fax: +1 604 684 5909.
E-mail addresses: mjakob@bgcengineering.ca (M. Jakob), Steve.Lambert@ec.gc.ca (S. Lambert).
[1] Tel.: +1 250 363 8241; fax: +1 250 363 8247.

0169-555X/$ – see front matter © 2008 Elsevier B.V. All rights reserved.
doi:10.1016/j.geomorph.2008.12.009

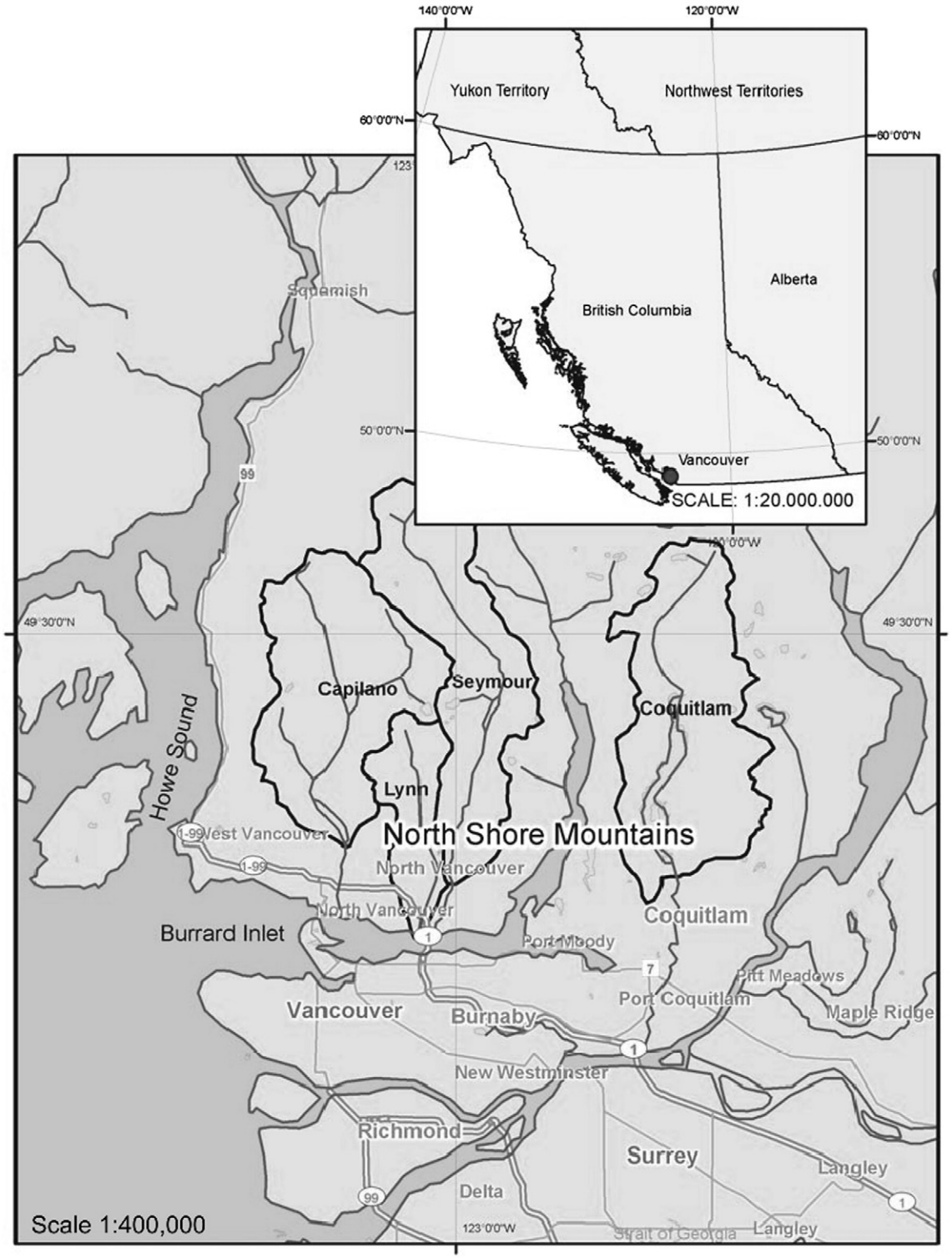

Fig. 1. Study area and locations mentioned in the text.

forest fires are rare and remain contained. The principal difficulty in predicting landslide response to climate change lies in predicting the magnitude of climate change and the response of various landslide types to the predicted change. This paper focuses exclusively on shallow landslides up to 1 m thickness, which are referred to as debris avalanche (Hungr et al., 2001), and debris flows (which typically evolve through channelization of debris avalanches).

The most important triggers of landslides in coastal British Columbia are prolonged rainfall followed by, or associated with, high intensity rainfall events (Jakob and Weatherly, 2003). Fig. 2 displays precipitation events that did trigger landslides on the North Shore Mountains, Howe Sound, and urban Vancouver over the past 40 years on a graph that relates antecedent precipitation (1 month accumulation) to the storm precipitation. The length of a given storm is variable, ranging from several hours up to 3 days, with an approximate median of 1 day. The 24-hour precipitation was thus used in subsequent analyses as a convenient surrogate for storm precipitation. The Howe Sound data suggest that a minimum of about 120 mm of antecedent

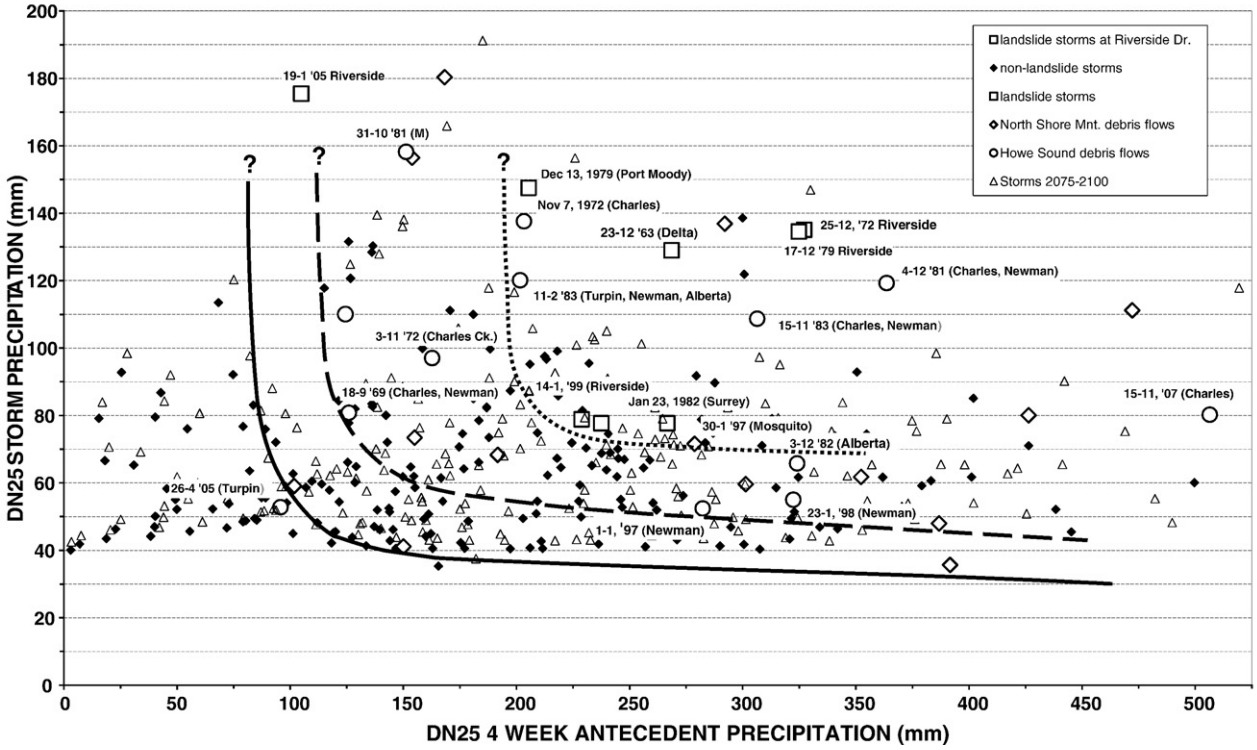

Fig. 2. Landslide envelopes for 24-hour storm rainfall and antecedent rainfall for urban landslides on Howe Sound and the North Shore Mountains.

rain measured in North Vancouver is necessary to overcome soil suction and establish soil moisture conditions that lend themselves to landslide activity once a critical rainfall intensity threshold has been exceeded (Jakob and Weatherly, 2003). Notably, however, the locally measured antecedent rainfall at a higher elevation may be significantly higher. Storm rainfall indicates that a minimum of about some 50 mm measured in North Vancouver is also required to trigger landslides. Because Howe Sound has no long-term rain gauges and none at higher elevations a local calibration cannot be achieved. A 40-year record from North Vancouver (station DN25) was also used to plot all storm rainfall events of 40 mm or more (black diamonds) to determine what proportion of such events likely triggered shallow landslides (Fig. 1). Thresholds were then added to indicate the lower limits of landslide-triggering antecedent and storm rain events for debris flows at Howe Sound, the North Shore Mountains and for urban landslides, many of which initiate in fill. Numerous nonlandslide-triggering storms (black diamonds) fall above the thresholds, which may either suggest that additional factors can trigger landslides, that the DN25 rain gauge does not calibrate well enough to the entire study area, or that some landslides may remain undetected in the more remote locations of the study area. Most likely a combination of all three factors play some role in explaining the nonperfect correlation shown in Fig. 1.

To predict landslide response to climate change, the first step is to try to predict changes in rainfall pattern. Two approaches lend themselves to estimating future changes in rainfall. The first is to extract trends from the observational record and then extrapolate those trends into the future. This method poses some problems. For example, it is difficult to isolate the secular trend from the data when being confounded by multi-year cyclical phenomena such as the El Niño Southern Oscillation (ENSO) and the Pacific Decadal Oscillation (PDO). In addition, trends from current data cannot be confirmed to persist into the future. For example, a study by Mote (2003) showed that the November to March mean precipitation trends in south-western British Columbia were noticeably stronger from 1900 to 1950 than from 1950 to 2000. If one had extrapolated the trend from the first half of the century to the second half, the result would have been seriously in error. The determination of trends in extreme precipitation is problematic. Stone et al. (2000) reported an overall increase in heavy rainfall frequency for spring, summer, and fall from 1950 to 1994. On the other hand, Zhang et al. (2001) reported little evidence of such a trend on a century timescale. In a comprehensive study of 14 tipping bucket rain gauges measuring at 5-minute intervals in the greater Vancouver area, Jakob et al. (2003) found no significant long-term trends for the 40 years of data they analysed for durations from 5 min to 24 h, suggesting that at least over the past four decades no persistent trend had emerged in the rainfall intensities.

The second approach that can be used to estimate future rainfall is to use the climate change simulations produced by global climate models (GCMs). These models are three-dimensional representations of the earth's climate system, in which physical processes governing climate are represented in mathematical terms. Such models can be used to simulate climatic conditions from the pre-industrial era (1850) into the future by assuming changes in atmospheric composition.

The physically based modelling approach is more easily defended than the statistically based extrapolation approach. In view of this, this study will be based primarily on the simulations of climate models. Two major classes of climate models can be differentiated: the first are relatively coarse-scale global models and the second are much finer scale regional climate models. The global-scale models, are much more common, and all the world's modelling groups perform global simulations in the course of their research activities. Such simulations are routinely made available to the scientific community. The situation for regional models is somewhat different. These models are run over much smaller regions, resulting in many fewer simulations being available for a given geographical area. In addition, the regional climate simulations are not as readily available for use by the scientific community.

The atmospheric composition is crucial in performing climate change experiments. In the past, modelling groups were at liberty to choose how the atmospheric composition changed in their simulations

making it difficult to compare the simulations available from a large number of climate models. In an attempt to standardize climate change simulations, the IPCC has developed several standard greenhouse gas emission scenarios that climate modellers use to perform their climate change experiments. The first group of six scenarios, termed IS92, were developed in 1992 for the IPCC Second Assessment Report (SAR) (Houghton et al., 1996) and are described in Leggett et al. (1992). These were followed in 1996 by 40 SRES (Special Report on Emissions Scenarios) described in the IPCC Third Assessment Report (TAR), (Houghton et al., 2001). The SRES are divided into four major families (A1, A2, B1, and B2) based on assumptions of population growth, use of technology, and economic growth. Some of these families contain more than one scenario. The rather large number of SRES prompted the IPCC to recommend that modelling groups perform climate change simulations for the Fourth Assessment Report (4AR) (IPCC, 2007) using primarily the B1, A1B, and A2 scenarios. These most recent simulations form the basis for the investigation presented here of landslide changes with global warming. From a climate modelling standpoint, the important features of each scenario are its greenhouse gas concentration and, to a lesser extent, its aerosol emissions. The evolution of the CO_2 concentrations and the SO_2 emissions for the more common scenarios are given in IPCC (2007) (Fig. 5 of the Summary for Policy Makers). The CO_2 concentrations vary considerably with each of the three scenarios. The scenario with the lowest increase in greenhouse gases is B1. Concentrations increase from present-day level to about 550 ppm in the year 2100. The *rate* of increase of CO_2 concentration *decreases* in time. The scenario with the next highest levels of CO_2 is A1B. Concentrations increase steadily from the present-day to about 720 ppm in 2100. The scenario with the strongest greenhouse gas forcing is A2, in which the CO_2 levels reach 840 ppm by 2100. The *rate* of increase of CO_2 concentration *increases* in time.

2. Reliability of climate models

Two methods are available to assess the reliability of climate models. The first of these is to have an ensemble of independent models perform identical climate change simulations. The results can simply be intercompared to ascertain the level of support for various aspects of the simulated climate change. Even though the possibility persists that a majority of the models are making the same type of error, increased agreement implies increased reliability.

Most modelling groups perform long simulations, generally beginning in pre-industrial times and extending well into the future. Such long runs provide another opportunity to examine the fidelity of climate models by comparing the so-called "present-day" segments of the simulations to currently available observations. Such comparisons made with a group of independent models have shown that the mean produced by averaging over all the models tends to exhibit a smaller departure from observations than any of the individual models. This observation is useful since it suggests that means computed over all the modelled climate change simulations appear to be a reasonable measure of the true conditions resulting from climate change.

Several shortcomings are inherent in climate models. Computer resources are finite, and this fact forces modelling groups to compromise on the formulation of the models. This is especially true for the resolution used for the simulations. Increasing the model resolution reduces the shortcomings of the model but dramatically increases the computing power needed. Modelling groups need to do multiple experiments with long simulations and this forces them to use modest resolution. The underlying assumption is that the small-scale features not taken into account by the relatively coarse models will have a relatively small effect on the large climatic scales that are important in climate changes studies. However, the absence of these small-scale structures in the climate simulations must be bourne in mind when evaluating the climates of GCMs.

3. Assessment of the current-day simulated precipitation

The precipitation-based factors favouring the occurrence of landslides are antecedent precipitation (which for the purposes of this study will be taken as the 28-day accumulated precipitation) and a relatively intense short-duration event (which is able to trigger a landslide if sufficient antecedent precipitation has fallen). We evaluate the 'present-day' simulations by comparing the statistics of 28-day and 1-day accumulations with those from observations. No attempt is made to distinguish between rain and snow as high 28-day and 1-day accumulations result primarily from rain because of their association with warm subtropical or tropical air masses, when the freezing level approaches or exceeds the highest peaks in the study area. Some error may be produced by the fact that at some elevation belts snow cover may exist that contributes to storm rainfall by melt.

Two classes of precipitation observations exist to assess climate model output. The first of these are observations at a single point, generally from rain gauges. Clearly, this type of estimate is subject to small-scale structures such as the distribution resulting from the small-scale features of topography. The second type is precipitation analyses. In the production of these analyses, the geographical region of interest is broken into analysis boxes that are usually latitude–longitude quadrangles. A sophisticated statistical technique is used to combine all available observations in a given box in order to produce a representative value for that box. The relatively large area of the analysis boxes results in an attenuation of small-scale features. This type of analysis is likely to be more flattering to the model simulations than point observations. However, because it is point values that trigger landslides (often cells of high intensity rainfall are embedded in or form because of orographic uplift and local wind pattern), both types of observations are used in the evaluation of the model.

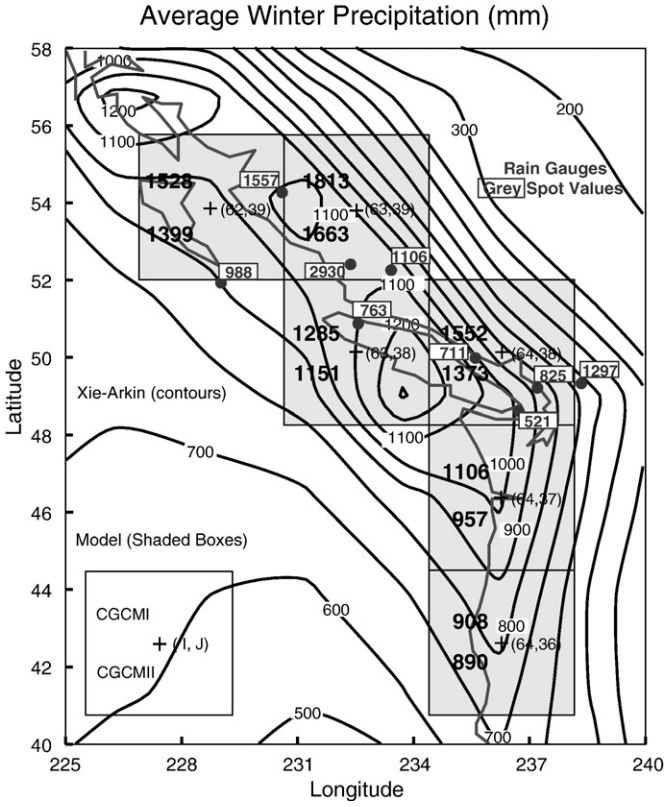

Fig. 3. The average winter precipitation simulated by CGCMI and CGCMII for the "current-day" climate. The left-hand values in the six shaded boxes give the model results in mm. The upper values refer to CGCMI and the lower values to CGCMII. The contoured field displays the analysed winter precipitation from Xie and Arkin (1997). The point values are the winter precipitation observations from rain gauges.

Table 1
Geographical coordinates of the rain gauge observation stations.

Station	Latitude (N)	Longitude (W)
Bella Coola	52° 20′	126° 38′
Cape St. James	51° 50′	131° 01′
Hope	49° 22′	121° 29′
Port Hardy	50° 41′	127° 22′
Powell River	49° 52′	124° 33′
Prince Rupert	54° 17′	130° 23′
Vancouver Airport	49° 11′	123° 10′
Vancouver Harbour	49° 18′	123° 07′
Victoria Gonzales	48° 25′	123° 19′

Daily precipitation output from the years 1900 to 2000 was available from two versions of the Canadian Centre for Climate Modelling and Analysis (CCCma) climate model, CGCMI and CGCMII. Three realizations were available from each model, making six "present-day" simulations available for analysis.

We begin the examination of the climate model simulations by considering the mean winter precipitation. Fig. 3 shows the region along and adjacent to the west coast of North America. The six shaded boxes are a portion of the atmospheric grid used by the model. The left side provides two values for the 100-year averaged precipitation for the respective box. The upper value is derived from CGCMI and the lower values from CGCMII. Each box also has an identification number to the right of the cross in the centre. The contoured field is the precipitation analysis of Xie and Arkin (1997). The analysis boxes (not shown) are 2.5° by 2.5° quadrilaterals. The rain gauge observations for locations with at least 50 years of observations are indicated by the green dots.

Fig. 3 shows that CGCMI simulates higher mean precipitation than does CGCMII. The Xie–Arkin contoured values exhibit a noticeable maximum along the coast. The values are about 700 mm off the coast of California and rise to about 1300 mm off Vancouver Island. Continuing northwestward, the values tend to decrease somewhat. Comparison with the model results shows reasonable accord for the four southernmost boxes, but the two northern boxes exhibit more precipitation than seen in the Xie–Arkin analyses. Rain gauge observations show the variation over areas the size of model grid squares. Generally, we can argue that when verified using the Xie–Arkin analyses the model has done a reasonable job in simulating the magnitude and geographical distribution of winter precipitation.

It was previously mentioned that localized (as opposed to large area averaged) precipitation is responsible for triggering landslides. Consequently, we continue the evaluation of the model output using only the rain gauge observations (the locations of the stations are listed in Table 1). The evaluation is done by constructing modelled and observed probability density functions (*pdfs*) for the 28-day and the 1-day accumulations. Probability density functions display the number of occurrences of given ranges of precipitation over the course of the simulation. Fig. 4 shows the *pdf* for the 28-day accumulated precipitation. The two bold curves are the model *pdfs*. The curve labelled "(63,39)" is for the model grid box over the lower mainland of British Columbia, and the curve labelled "(64,38)" is for the box centred over northern Vancouver Island (see Fig. 2). Considerable variation prevails in the observation-based *pdfs*. With the exception of three locations, which are in rain shadows (Victoria, VR Airport, and Powell River), the modes of the simulated precipitation agree well with the observed modes of precipitation. This result suggests that the

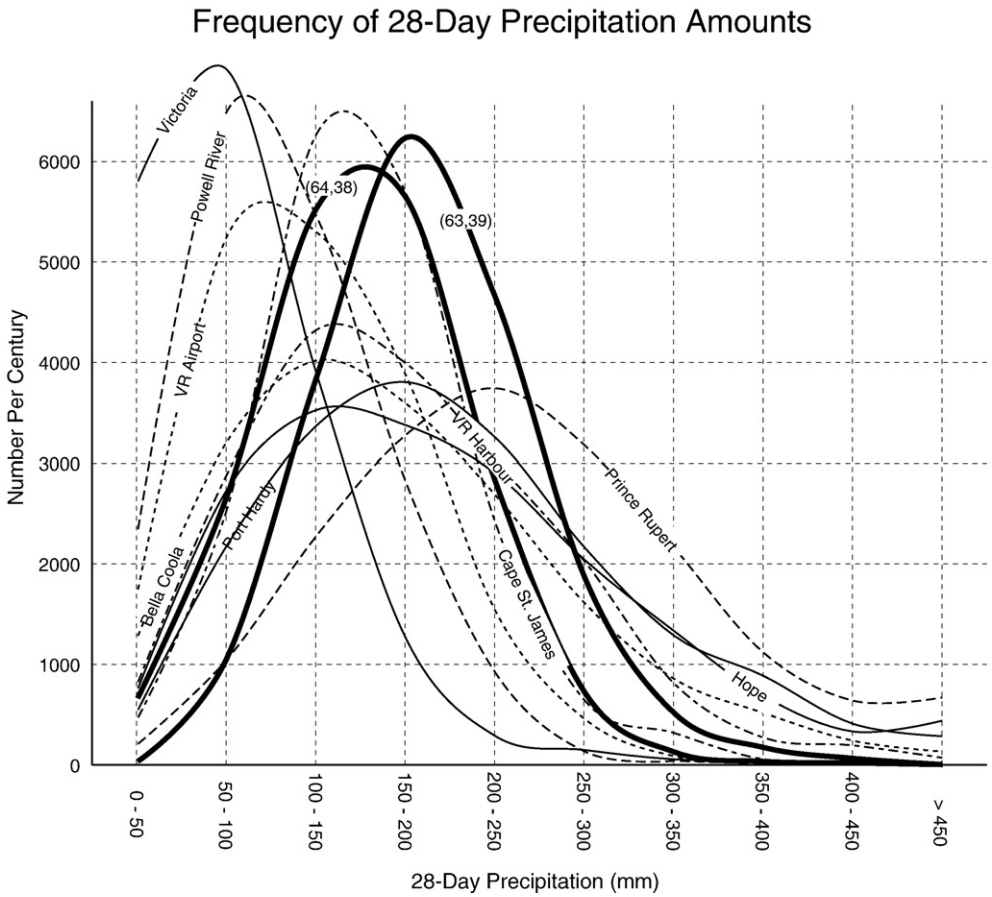

Fig. 4. The probability density functions (*pdfs*) for the 28-day precipitation. The bold curves give the mean model result averaged over the six present-day simulations. The curve labelled "(64,38)" gives the result for the (64,38) grid square shown on Fig. 2, and the curve labelled "(63,39)" the results for the (63,39) grid square.

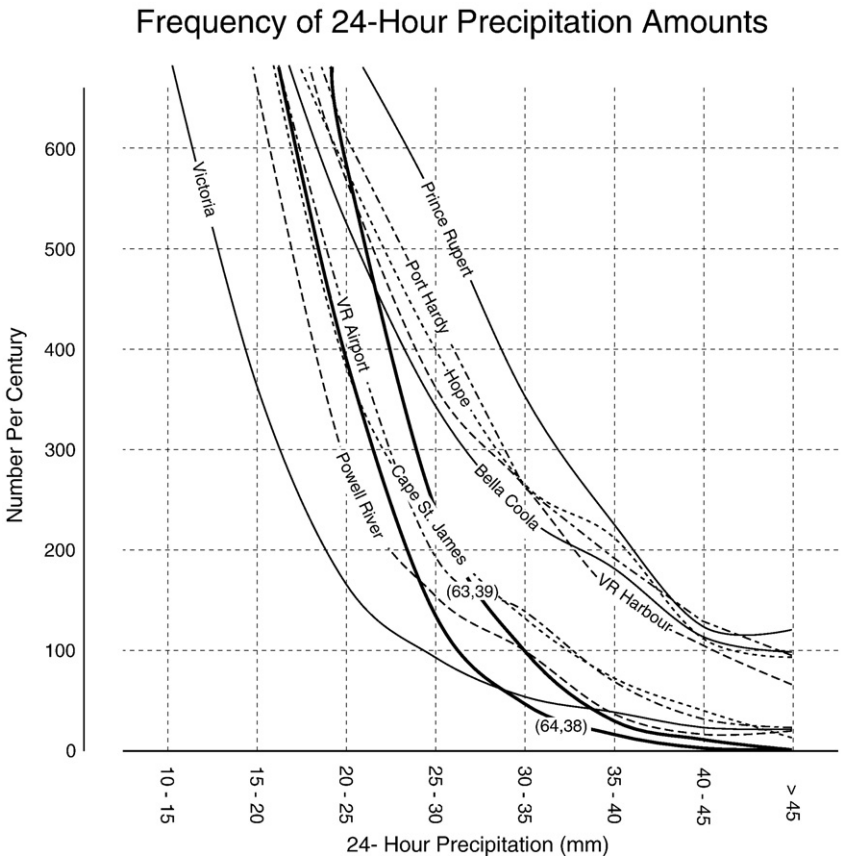

Fig. 5. Same as Fig. 2 except for 24-hour precipitation.

models are able to simulate the antecedent precipitation criterion for the occurrence of landslides.

We now include the 1-day accumulated precipitation. Because short-term events will be more sensitive to the coarse resolution, we expect that the agreement between the observed *pdfs* and the modelled *pdfs* will be poorer than those for the 28-day accumulations. Fig. 5 shows the upper tail (right-hand side) of the *pdf* for the 1-day accumulations. The modelled frequencies of the large accumulations (>35 mm/d), those favourable to landslide occurrence, are much less than the corresponding observed frequencies. In spite of this poor

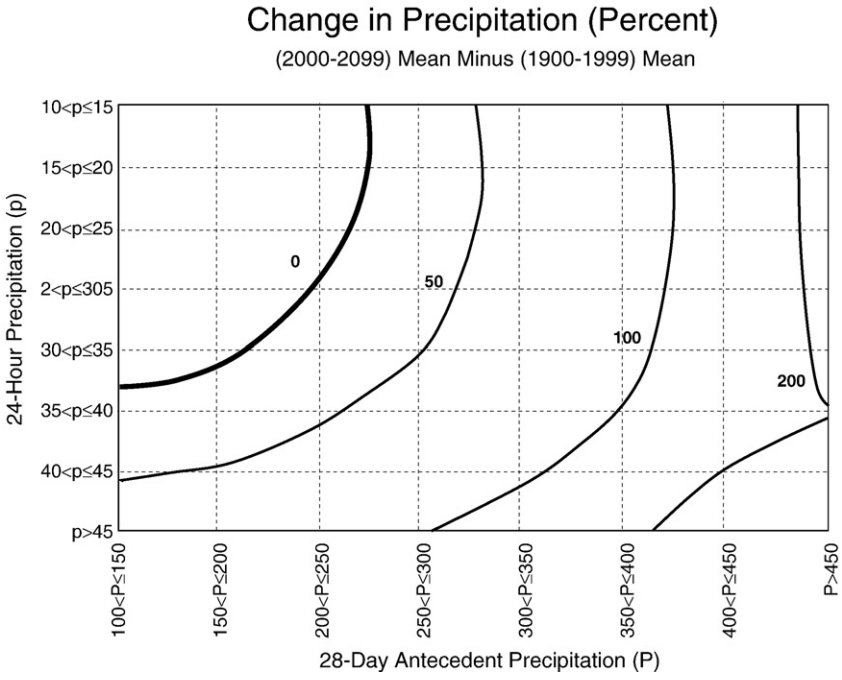

Fig. 6. The percentage changes in frequencies of the 28-day and the 1-day precipitation amounts for the period 2000–2099 compared to the period 1900–1999.

agreement, we can postulate that this result might nonetheless be useful in inferring relative changes in landslide frequency with global warming. We assume that the lack of agreement is the result of the coarse resolution model that fails to take into account microscale processes such as orographically enhanced rainfall intensities. This shortcoming of the model should be relatively independent of the type of simulation and likely would be present in both the "present-day" and in the enhanced warming simulations. Even though the absolute values of the 1-day precipitation are weaker than observed, it should still be possible to obtain an indication of how the 1-day precipitation will change in a warmer climate by comparing the 1-day statistics from the current day and enhanced warming simulations.

4. Precipitation changes with global warming

We first examine the simulated changes in precipitation for the twenty-first century for the mean of the six realizations of CGCMI and CGCMII. Fig. 6 shows the percentage changes in frequency of both the 28-day and the 1-day precipitation accumulation for grid box (64,38), obtained by subtracting the current day (1900–1999) means from the climate change (2000–2099) means. Generally, the 28-day accumulation and the 1-day accumulation increase with global warming, with the increase being proportionally larger with increasing accumulations. This prediction clearly promotes favourable conditions for increased landslide potential along the southern coast during the next century.

Table 3
The percentage increase in precipitation for 2071–2100 compared to 1961–1990 simulated by various models using three SRES scenarios.

Scenario									
	B1			A1B			A2		
Model	SON	DJF	AW	SON	DJF	AW	SON	DJF	AW
BCM2.0	8.4	−1.1	3.7	23.1	3.7	13.4	23.5	7.6	16.6
CGCM3T47	36.7	−9.4	13.7	13.4	5.8	9.6	24.3	16.3	20.3
CNRMCM3	23.5	3.1	13.3	38.9	20.2	29.6	42.2	20.7	31.5
CSIROMk3	6.4	16.2	11.3				20.5	22.7	21.6
ECHAM5OM	2.1	15.5	8.8	10.9	6.4	8.7	3.4	10.6	7.0
ECHO-G	13.8	5.6	9.7	15.0	7.7	11.4	20.6	4.1	12.4
GFDLCM2.0	12.9	11.1	12.0	3.5	16.0	9.8	2.6	14.5	8.6
GFDLCM2.1	2.9	4.8	3.9	1.4	0.8	1.1	−0.9	2.4	0.8
GISSAOM	16.0	3.1	9.6	26.7	9.8	18.3			
GISSE-H				−22.2	6.5	−7.9			
GISSE-R	−1.5	5.5	2.0				15.5	2.3	8.9
HADCM3	11.9	1.9	6.9	3.9	−2.7	0.6	−1.1	8.3	3.6
HADGEM1				3.6			−4.9		
INMCM3.0	3.7	21.4	12.6	6.4	14.0	10.2	2.1	27.4	14.8
IPSLCM4	18.8	22.8	20.8	35.6	27.9	31.8	24.2	30.9	27.6
MIROC-hires	16.2	9.3	12.8	20.8	20.3	20.6			
MIROC-medres	20.7	16.9	18.8	27.4	13.5	20.5	21.9	21.8	21.9
NCARCSM3	−0.9	−1.5	−1.2	1.8	−0.7	0.6	5.0	−2.8	1.1
NCARPCM				−11.1	16.5	2.7	−2.0	5.9	2.0
Model mean	12.0	7.8	9.9	11.7	10.4	11.1	12.3	10.6	11.5

The columns 'SON' give the increases for September to November, 'DJF' gives the changes for December to February, and AW gives the increases for September to February. The row labelled "Model mean" is the average over all the models.

Table 2
Models for which output was available.

Model	Country	Horizontal grid	Documentation
BCM2.0	Norway	128×64	http://www.pcmdi.llnl.gov/ipcc/model_documentation/BCCR_BCM2.0.htm
CGCM3T47	Canada	96×48	http://www.cccma.ec.gc.ca/models/cgcm3.shtml
CNRMCM3	France	128×64	http://www.pcmdi.llnl.gov/ipcc/model_documentation/CNRM-CM3.htm
CSIROMk3	Australia	192×96	http://www.pcmdi.llnl.gov/ipcc/model_documentation/CSIRO-Mk3.0.htm
ECHAMO5	Germany	192×96	http://www.pcmdi.llnl.gov/ipcc/model_documentation/ECHAM5_MPIOM.htm
ECHO-G	Germany Korea	96×48	http://www.pcmdi.llnl.gov/ipcc/model_documentation/ECHO-G.htm
GFDLCM2.0	U.S.A.	144×90	http://www.pcmdi.llnl.gov/ipcc/model_documentation/GFDL-cm2.htm
GFDLCM2.1	U.S.A.	144×90	http://www.pcmdi.llnl.gov/ipcc/model_documentation/GFDL-cm2.htm
GISSAOM	U.S.A.	90×60	http://www.pcmdi.llnl.gov/ipcc/model_documentation/GISS-AOM.htm
GISSE-H	U.S.A.	72×46	http://www.pcmdi.llnl.gov/ipcc/model_documentation/GISS-E.htm
GISSE-R	U.S.A.	72×46	http://www.pcmdi.llnl.gov/ipcc/model_documentation/GISS-E.htm
HADCM3	U.K.	96×72	http://www.pcmdi.llnl.gov/ipcc/model_documentation/HadCM3.htm
HADGEM1	U.K.	192×144	http://www.pcmdi.llnl.gov/ipcc/model_documentation/HadGEM1.htm
INMCM3.0	Russia	72×45	http://www.pcmdi.llnl.gov/ipcc/model_documentation/INM_CM3.0.htm
IPSLCM4	France	96×73	http://www.pcmdi.llnl.gov/ipcc/model_documentation/IPSL-CM4.htm
MIROC-hires	Japan	320×160	http://www.pcmdi.llnl.gov/ipcc/model_documentation/MIROC3.2_hires.htm
MIROC-medres	Japan	128×64	http://www.pcmdi.llnl.gov/ipcc/model_documentation/MIROC3.2_medres.htm
NCARCSM3	U.S.A.	256×128	http://www.pcmdi.llnl.gov/ipcc/model_documentation/CCSM3.htm
NCARPCM	U.S.A.	128×64	http://www.pcmdi.llnl.gov/ipcc/model_documentation/PCM.htm

The 'Horizontal grid' column lists the number of rows and columns of the global grid on which the precipitation data were available and is a measure of the resolution of the model.

Little basis exists to make definitive statements concerning the reliability of future climates predicted by climate models. As mentioned previously, one method is available to examine simulations of many independent climate models to verify if there is a consensus among them. A wide variety of output from many climate models used to support the production of the IPCC assessment reports is available at the website, http://www.cccsn.ca/. Monthly mean precipitation data from 19 models used in the most recent IPCC 4AR are available for the 2071–2100 period. For the 4AR report, the modelling groups were asked to concentrate on three SRES scenarios; B1, A1B, and A2. Each of these scenarios assumes a different concentration of greenhouse gases. In the year 2100, the greenhouse gas concentration used in the B1 scenario is about 550 ppm, in the A1B scenario 720 ppm, and in the A2 scenario 840 ppm. Table 2 lists the models for which precipitation output was available. Because only monthly mean data are available, it is not possible to compare the short-term rainfall from the models (the problem of the lack of short-term precipitation will be addressed in a subsequent section).

Seasonal model precipitation means were extracted for south-western British Columbia. The simulated values for each model grid box that contained the point "(123 W,49 N)" were used to investigate the changes in rainfall with global warming. Table 3 provides the percentage increase in precipitation simulated by the models for the period 2071–2100 compared to the period 1961–1990 for each of the three scenarios. The columns labelled "SON" give the mean autumn (September–October–November) results, the columns labelled "DJF" give the winter (December–January–February) results, and the columns labelled "AW" give the means over the autumn plus winter seasons. The results show that despite considerable variability in the simulations, a strong qualitative consensus persists. In general, all models predict that the seasonal rainfall for the fall and winter months will increase with global warming. If we consider that the results are composed of the desired climate change signal upon which a random component is superimposed, then we can attempt to isolate the climate signal by computing the mean over all the models. This is also included in Table 3. As a group, the models predict that the autumn season rainfall will increase more than the winter season rainfall. This is a particularly relevant result because the highest

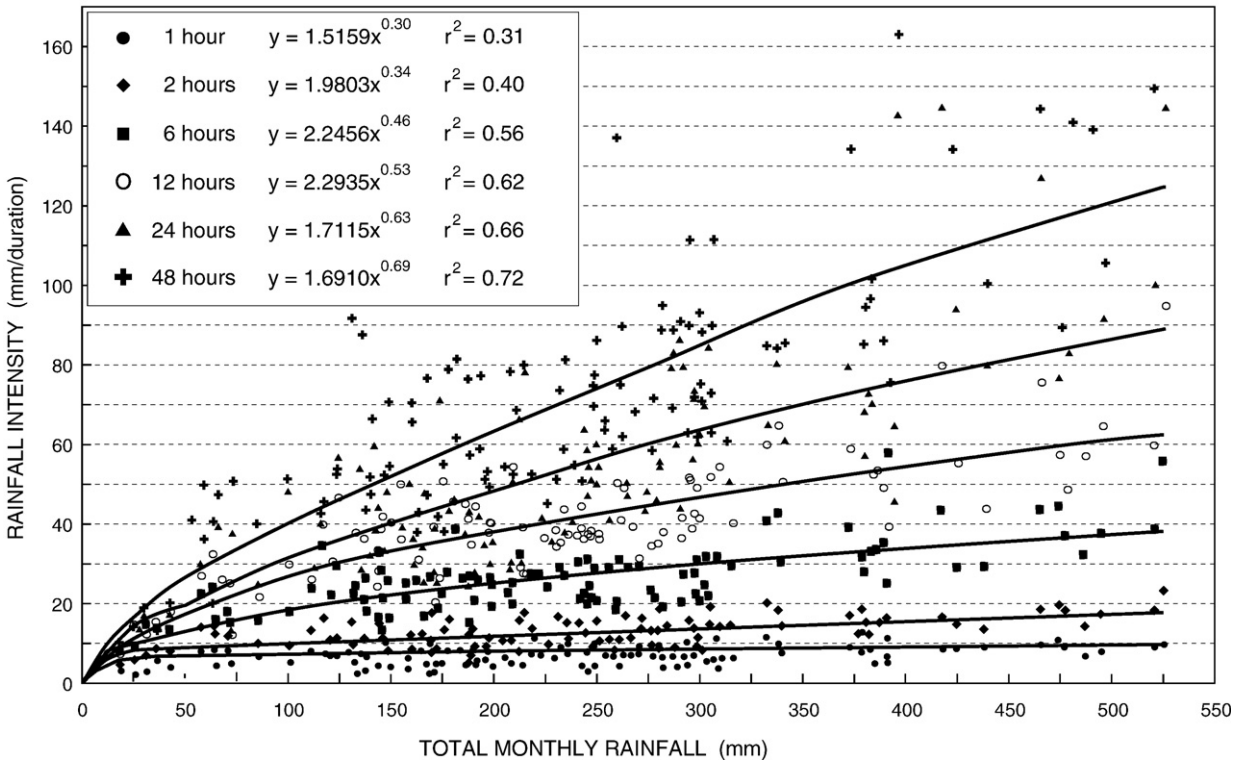

Fig. 7. Rainfall intensity versus total monthly rainfall for North Vancouver.

landslide frequency along the southwest coast of British Columbia occurs during autumn.

One may expect that simulations that use a higher concentration of greenhouse gases should also exhibit larger increases in precipitation. This behaviour is seen in the "AW" values for the model means: the A2 scenario results in the largest precipitation increase, while the B1 scenario gives the smallest increase. This is an encouraging result because it indicates that the model simulations are mutual consistent and that this fact increases the confidence in the model results.

The model consensus is that precipitation will increase during fall and winter with the average increase being about 10% by the end of the twenty-first century. This should provide more favourable base line soil saturation conditions compared to the present day and should translate into a higher probability of regional landsliding even if other landslide triggers, such as short-term rainfall, remain unchanged.

Current climate models have difficulty in reproducing the statistics of the short-term precipitation but do seem able to produce reasonable simulations of the antecedent (monthly) rainfall. This necessitates the use of a statistical technique to relate the short-term rainfall to monthly rainfall. Miles and Associates (2001) compared annual rainfall and rainfall intensities and found good correlations for a large number of stations for return periods between 2 and 100 years. This result suggests that a correlation between short-term precipitation and monthly precipitation may prove useful. Fig. 7 shows the short-term rainfall amounts observed at North Vancouver over periods of 1 to 48 h plotted against the total monthly rainfall. In order to extract a relation between the short-term precipitation and the monthly precipitation, power law curves of the following form are fitted to the data:

$$P_{\text{short}} = AP_{\text{month}}^{K} \tag{1}$$

where P_{short} is the short-term precipitation; and P_{month} is the monthly precipitation; and A, K are parameters obtained by fitting Eq. (1) to the data.

This relationship can be manipulated to express fractional changes in the short-term precipitation as a function of fractional changes in the monthly precipitation; i.e.,

$$\frac{\Delta P_{\text{short}}}{P_{\text{short}}} = K\frac{\Delta P_{\text{month}}}{P_{\text{month}}} \tag{2}$$

The curves in Fig. 7 show the power law fit for various short-term precipitation periods and the inset of the figure gives the resulting equation and the variance explained for each of the short-term accumulation periods. Except for very short rainfall intensity periods (1 and 2 h), the fitted curves explain most of the variance, suggesting that there is a fairly robust relationship between changes in monthly precipitation and changes in short-term rainfall; i.e., increased monthly precipitation results in increased short-term precipitation. The curve-fitting procedure was applied to two other locations, West Vancouver and Squamish, and produced similar results. Interestingly, Fig. 7 suggests that the magnitude of change will also increase with increasing rainfall duration (exponent increase from 0.30 for 1-hour rainfall to 0.69 for 48-hour rainfall). Table 4 shows the results for the

Table 4
The power law equations relating 24-hour rainfall to monthly rainfall for three locations in south-western British Columbia.

		West Vancouver	North Vancouver	Squamish
January	Equ.	$y = 0.192x^{1.050}$	$y = 0.75x^{0.790}$	$y = 0.55x^{0.849}$
	r^2	0.47	0.68	0.92
October	Equ.	$y = 2.99x^{0.539}$	$y = 1.39x^{0.684}$	$y = 6.50x^{0.417}$
	r^2	0.62	0.79	0.81
November	Equ.	$y = 0.904x^{0.751}$	$y = 5.02x^{0.433}$	$y = 1.57x^{0.664}$
	r^2	0.65	0.46	0.70
December	Equ.	$y = 0.778x^{0.759}$	$y = 1.31x^{0.675}$	$y = 0.66x^{0.819}$
	r^2	0.47	0.74	0.41
October–January	Equ.	$y = 2.16x^{0.592}$	$y = 1.71x^{0.633}$	$y = 1.45x^{0.680}$
	r^2	0.54	0.66	0.84

24-hour short-term precipitation. The regression equation and the percentage of variance explained at each of the three locations are given for the months from October to January.

The multimodel climate change simulation results presented previously showed an average increase of slightly over 10% during the twenty-first century when the results are averaged over all models and the three scenarios. According to Eq. (2), changes in the short-term precipitation are related to changes in the antecedent precipitation scaled by the exponent K of Eq. (1). From the "landslide season" results of Table 4 (Oct–Jan), the exponents range from 0.59 to 0.68. If the statistical relation holds for the modelled data, then global warming should lead to a slightly larger than 6% increase in the short-term (24 h) precipitation. Consequently, the modelling results indicate that global warming should result in a precipitation regime more favourable to landslides in southwestern British Columbia.

5. Changes in landslide occurrence

Landslides are triggered through a combination of hydroclimatic factors. This paper has re-emphasized that in the coastal mountains of British Columbia a combination of antecedent moisture conditions and rainfall intensity best explains the temporal occurrence of landslides.

The previous section suggests that, on average, a 10% increase in 4 week antecedent rainfall and a 6% increase in 24-hour precipitation can be expected by the end of the next century. While this information suggests that landslides may occur more frequently, it does not provide guidance on the magnitude of that increase.

Fig. 2 shows storms that did, and did not, trigger landslides exceeding 40 mm of rainfall as measured in North Vancouver. The horizontal axis denotes the 4 week antecedent rainfall, while the vertical axis shows storm rainfall that can be approximated to 24-hour intensity as most heavy rainfall events last about 1 day. Accordingly, each datapoint of non-landslide triggering storms can be adjusted by 10% (horizontal axis) and 6% (vertical axis), respectively for a hypothetical period between the years 2075 and 2100. This procedure allows the calculation of a change in landslide occurrence for specific regions. Debris flows occurring on creeks along the Howe Sound east shores will serve as an example.

A total of 75 storms plot above the debris flow initiation threshold shown in Fig. 2. Of those, 12 storms are known to have triggered debris flows in the past 25 years, which corresponds to a 15% proportion of storms leading to debris flows. Climate change and associated alterations in the precipitation regime would raise the total number of storms above the Howe Sound debris flow threshold to 96 events. It is then reasonable to assume that the proportion of storms triggering debris flows to remain constant at 15%, which would result in an expected 15.4 debris flows in a period from 2075 to 2100. This corresponds to a 28% increase in debris flow occurrence assuming that all other factors (i.e. degree of forest cover, landuse, type and distribution of tree cover, forest fire frequency) remain constant.

While a 28% increase in the number of debris flows for Howe Sound in the course of a century sounds substantial, it pales in comparison with changes in landslide activity due to poor logging practices and associated road building. For example, logging on the Queen Charlotte Islands and Clayquot Sound have increased spatial landslide density by factors of 12 and 9, respectively (Schwab, 1983; Jakob, 2000). At Howe Sound as well as most debris flow-prone areas in the Coast Mountains, debris flow channels are well defined. An increase in the total number of debris flows will thus result in an increased frequency of debris flows in each channel. Since most of the debris flow channels along Howe Sound are weathering-limited, a higher frequency of debris flows may result in a decreased volume per event (Bovis and Jakob, 1999; Jakob et al., 2005). At this point, however, changes in landslide frequency–magnitude relationships as a consequence of climate change are still highly speculative.

6. Summary and conclusions

The effect of global warming on the relative frequency of landslides along the British Columbia coast is studied by examining the monthly mean simulations of precipitation from 19 climate models using three IPCC climate change scenarios.

We first attempted to assess the reliability of climate models by comparing simulations for the current-day climate along the British Columbia coast using two versions of the CCCma model (CGCMI and CGCMII) for which daily data were available. Comparison of the model output to current-day observations showed that the model was reasonably successful in simulating the antecedent precipitation but was less successful in simulating the short-term precipitation, presumably because of the models' coarse resolution.

Subsequently, the simulations for the end of the twenty-first century from 19 climate models were examined to determine the effect of global warming on the antecedent precipitation. Averaged over all the models and the three scenarios, the increase in antecedent precipitation was slightly over 10%. In spite of the fact that there is a great deal of intermodel variability, the models agree rather well in a qualitative sense in that there are very few simulations that show a decrease in precipitation and that an increase in greenhouse gas concentration leads to increased precipitation change.

Finally, to overcome the model problems in simulating short-term precipitation intensities, a statistical technique was employed to relate the short-term precipitation change to total monthly rainfall changes. This statistical result suggested that the short-term precipitation would increase by slightly over 6% by the end of the century.

Given that the antecedent precipitation and the short-term precipitation are important triggers for landslides and that the models predict increases in both of these quantities, it is reasonable to expect that landslide frequency along the southwest coast of British Columbia will increase during the twenty-first century.

For specific areas it will be possible to estimate the total number of landslides based on the proportion of storms that have triggered landslides and those that have not. At Howe Sound, for example, the total number of debris flows may increase by approximately 30% by the end of the century.

Acknowledgments

BGC Engineering Inc. and the Canadian Centre for Climate Modelling and Analysis supported this study. Bill Taylor of Environment Canada provided useful comments to an earlier draft. The Geological Survey of Canada provided the original impetus for this study in the form of a small consulting assignment on landslides and climate change along the Sea to Sky corridor.

References

Bovis, M.J., Jakob, M., 1999. The role of debris supply to determine debris flow activity in southwestern B. C. Earth surf. processes landf. 24, 1039–1054.

Houghton, J.T., Meiro Filho, L.G., Callender, B.A., Harris, N., Kattenburg, A., Maskell, K. (Eds.), 1996. Climate Change. The Science of Climate Change. The Second Assessment of the Intergovernmental Panel on Climate Change. Cambridge University Press, Oxford, UK. 572 pp.

Houghton, J.T., Ding, Y., Griggs, D.J., Noguer, M., van der Linden, P.J., Dai, X., Maskell, K., Johnson, C.A. (Eds.), 2001. Climate Change 2001. The Scientific Basis. Cambridge University Press. 881 pp.

Hungr, O., Evans, S.G., Bovis, M.J., Hutchinson, J.N., 2001. A review of the classification of landslides in the flow type. Environ. eng. geosci. VII (3), 221–228.

Intergovernmental Panel on Climate Change (IPCC), 2007. Climate change 2007: the physical science basis. Contribution of Working Group I to the fourth assessment report of the intergovernmental panel on climate change. In: Solomon, S., Qin, D., Manning, M., Chen, Z., Marquis, M., Avery, K.B., Tignor, M., Miller, H.L. (Eds.), Fourth Assessment Report. Cambridge University Press, Cambridge, UK, and New York, USA. 996 pp.

Jakob, M., 2000. The Impacts of Logging on Landslide Activity at Clayoquot Sound, vol. 38. Catena, Vancouver Island, BC, pp. 279–300.

Jakob, M., Weatherly, H., 2003. A Hydroclimatic Threshold for Landslide Initiation on the North Shore Mountains of Vancouver, British Columbia. Geomorphology, vol. 54, pp. 137–156.

Jakob, M., McKendry, I., Lee, R., 2003. Changes in rainfall intensity in the Greater Vancouver Regional District, British Columbia. Can. water resour. j. 28 (4), 587–604.
Jakob, M., Bovis, M., Oden, M., 2005. Estimating debris flow magnitude and frequency from channel recharge rates. Earth surf. processes landf. 30, 755–766.
Leggett, J., Peppwe, W., Swart, R., 1992. Emissions scenarios for the IPCC: an update. In: Houghton, J., Callander, B., Varney, S. (Eds.), Climate Change 1992: The Supplementary Report to the IPCC Scientific Assessment. Cambridge University Press, United Kingdom, pp. 69–95.
Miles and Associates, 2001. Effects of Climate Change on the Frequency of Slope Instabilities in the Georgia Basin, BC — Phase 1. Canadian Climate Action Fund Project Number A160. 39 pp.
Mote, P.W., 2003. Twentieth-century fluctuations and trends in temperature, precipitation, and mountain snowpack in the Georgia Basin—Puget Sound Region. Can. water resour. j. 28, 567–585.
Stone, D.A., Weaver, A.J., Zwiers, F.W., 2000. Trends in Canadian precipitation intensity. Atmos.-ocean 38, 321–347.
Xie, P., Arkin, P.A., 1997. Global precipitation: a 17-year monthly analysis based on gauge observations, satellite estimates, and numerical model outputs. Bull. Am. Meteorol. Soc. 78, 2539–2558.
Zhang, X., Hogg, W.D., Mekis, E., 2001. Spatial and temporal characteristics of heavy precipitation events over Canada. J. Climate 14, 1923–1935.